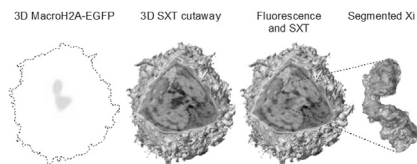


(CCFT-SXT). Correlation of these two three-dimensional datasets was performed using fiducial markers visible in both modalities. The Xi was identified in each cell by its strong enrichment in a fluorescently-labeled histone variant, macroH2A-EGFP. We present the overall topology, compaction profile, and volume occupied by the Xi in interphase nuclei. Physical contacts with nucleoli and the nuclear envelope are also described. Examination of eleven individual cells showed that there is considerable variation in the spatial arrangement and compaction profile adopted by the Xi.



2198-Plat

Observation of the Change of Synapses After Long-Term Potentiation Induction using Super-Resolution Imaging

Sang Hak Lee^{1,2}, En Cai^{1,2}, Okunola Jeyifous³, Michelle A. Baird⁴, Michael W. Davidson⁴, William N. Green³, Paul R. Selvin^{1,2}.

¹University of Illinois at Urbana-Champaign, Urbana, IL, USA, ²Center for the Physics of Living Cells, University of Illinois at Urbana-Champaign, Urbana, IL, USA, ³University of Chicago, Chicago, IL, USA, ⁴Florida State University, Tallahassee, FL, USA.

Synapses are the fundamental structures for signal transmission in neurons. A synapse is a cell-cell junction composed of pre-synapse and post-synapse between neurons. The structure of synapses is dynamically changing upon external stimuli. In this work, we used super-resolution imaging technique (PALM) to study the synaptic changes after inducing long-term potentiation (LTP). In particular, after LTP induction, we investigated the changes in distances between 1. A presynaptic protein (synapsin and postsynaptic scaffold proteins (Homer1 and PSD95) and 2. Two different postsynaptic scaffold proteins, namely Homer1 and PSD95. We labeled these proteins using photo-activable proteins such as mEOS2, Dronpa, and mGeos, and obtained two-color PALM imaging for each pair of synaptic proteins. Chromatic aberration was corrected for a more precise measurement of the distances. We found out that, after LTP induction, the distance between Homer1 and PSD95 decreased significantly from 330 nm to 90 nm; the distance between synapsin and PSD95 also decreased from 243 nm to 125 nm. Moreover, we carried out fast PALM imaging, which allows us to take super-resolution images every minute, in order to observe the volume change of synapses during LTP. Observation of the time-dependent distribution of PSD95 and Homer1 has shown that the average volume of synapses is increasing after LTP induction from 0.05 μm^3 to 0.076 μm^3 .

2199-Plat

Single-Molecule Fluorescence Imaging Reveals Mismatch Repair Dynamics in Live *Bacillus Subtilis*

Yi Liao¹, Jeremy W. Schroeder², Lyle A. Simmons², Julie S. Biteen¹.

¹Chemistry, University of Michigan, Ann Arbor, MI, USA, ²Molecular, Cellular and Developmental Biology, University of Michigan, Ann Arbor, MI, USA.

The error-free progression of DNA replication is essential for all organisms, and deficiencies in DNA repair mechanisms can have severe consequences, from increased antibiotic resistance in bacteria to human cancers. The mismatch repair (MMR) pathway corrects base-pairing errors that are incorporated during genome replication. This pathway is critical for maintaining genomic fidelity: loss of MMR increases the mutation rate several hundred-fold in bacteria and humans alike. From prokaryotes to human cells, the highly conserved MMR protein MutS and its homologs recognize mismatched nucleotides and recruits downstream MMR proteins for repair. Despite the crucial role of MutS in MMR, the mechanism by which MutS first locates base-pairing errors remains unclear.

We have developed new methods of super-resolution imaging to reveal the in vivo single-molecule distributions and dynamics of MutS in live *Bacillus subtilis*. This Gram-positive bacterium has served as the model for studying DNA replication and repair due to its genetic competence and high homology with corresponding pathways in humans. Based on Photoactivated Localization Microscopy (PALM) and single-particle tracking (SPT), we localized and tracked MutS-PAmCherry and the replisome subunit DnaX-mCitrine with 20-nm precision to reveal the spatial relationship and diffusive behaviors of these two proteins. We observed transient, mismatch-dependent colocalization between MutS-PAmCherry and DnaX-mCitrine with two-color PALM imaging, and SPT revealed dramatic changes in MutS-PAmCherry diffusion rates and confinement behavior upon mutagen treatment. To develop a mechanistic understanding, we have studied wt MutS as well as mutant strains defective for mismatch recognition and mismatch unbinding, respectively, and studied

how the interactions between MutS-PAmCherry and the replisome are changed by such mutations. Together, our results provide strong evidence supporting that MutS recruitment to the replisome is required for MMR and precedes mismatch binding events in vivo.

2200-Plat

Subdiffraction Imaging Reveals Molecular Architecture at the Transition Zone of Primary Cilia

T. Tony Yang¹, Won-Jing Wang², Arthi Suresh¹, Meng-Fu Bryan Tsou², Jung-Chi Liao^{1,3}.

¹Mechanical Engineering, Columbia University, New York, NY, USA, ²Cell Biology Program, Memorial Sloan-Kettering Cancer Center, New York, NY, USA, ³Biomedical Engineering, Columbia University, New York, NY, USA. Recent studies have identified important regulating elements for transition zone (TZ) gating in cilia. However, the architecture of the TZ region and its arrangement relative to intraflagellar transport (IFT) proteins remain largely unknown, hindering the mechanistic understanding of the regulation mechanisms. One of the major challenges comes from the tiny volume at the ciliary base packed with numerous proteins, with the diameter of the TZ close to the diffraction limit of conventional microscopes. Using a custom-built stimulated emission depletion (STED) superresolution microscope, we revealed relative localizations of TZ proteins, IFT proteins, transition fiber (TF) proteins, and centriole proteins. We found TCTN2 at the outmost periphery of the TZ close to the ciliary membrane, with a 227 ± 18 nm diameter. TMEM67 was adjacent to TCTN2, with a 205 ± 20 nm diameter. RPGRIP1L was localized toward the axoneme at the same axial level as TCTN2 and TMEM67, with a 165 ± 8 nm diameter. Surprisingly, CEP290 (antibody against C-terminal amino acids) was localized at the proximal side of the TZ close to the distal end of the centrin-labeled basal body. The lateral width was unexpectedly close to the width of the basal body, distant from the potential Y-links region of the TZ. IFT88 was also surprisingly distributed in two distinct patterns, forming three puncta or a Y shape at the ciliary base. We hypothesize that the two distribution states of IFT88 correspond to the open and closed gating states of the TZ, where IFT particles aggregate to form three puncta when the gate is closed, and move to form the branches of the Y-shape pattern when the gate is open.

2201-Plat

Super-Resolution Imaging of Telomeres Reveals that Compaction of Telomeric DNA by Shelterin Protects Chromosome Terminii

Jigar N. Bandaria¹, Veysel Berk², Steven Chu², Ahmet Yildiz¹.

¹Physics and Molecular and Cell Biology, University of California, Berkeley, CA, USA, ²Physics and Molecular and Cellular Physiology, Stanford University, Stanford, CA, USA.

Telomeres, which are tandem TTAGGG repeats at the ends of mammalian chromosomes, are susceptible to degradation by nucleases and misrecognition as breaks in DNA. Telomeres are protected against DNA damage response (DDR) pathways by the shelterin complex. It has been proposed that higher order remodeling of telomeric chromatin by shelterin plays a role in this protection, but telomeres cannot be studied by crosslinking and chromosome capture methods due to failure of sequence discrimination between repetitive TTAGGG tracts. Using photoactivated localization microscopy (PALM) we imaged telomeres in human cells at ~ 15 nm of resolution. We found that shelterin mediates formation of compact telomeric structures (~ 150 nm in diameter). Knockdown of TRF1, TRF2 and TIN2 subunits of shelterin results in decompaction and up to 30-fold increase in volume of these telomeric structures. Mutations that abrogate TRF1 or TRF2 dimerization also lead to different levels of telomere decompaction, which positively correlates with DDR signal accumulation at telomeres in these cells. The changes in telomere structure are not due to DDR accumulation in TRF2 mutant cells, because similar levels of decompaction are observed after inactivating the ataxia telangiectasia mutated (ATM) pathway using RNAi. Our results demonstrate that shelterin remodels telomeric chromatin into compact structures by inter-repeat crosslinking of telomeric tracts.

2202-Plat

Live 4D Imaging of the Embryonic Vertebrate Heart with Two-Photon Light Sheet Microscopy and Simultaneous Optical Phase Stamping

Thai V. Truong¹, Vikas Trivedi², Le Trinh¹, Daniel Holland¹, Francesco Cutrale¹, John M. Choi¹, Scott E. Fraser¹.

¹Translational Imaging Center, University of Southern California, Los Angeles, CA, USA, ²Bioengineering, California Institute of Technology, Pasadena, CA, USA.

The developing vertebrate heart is a highly dynamic organ that starts to function early on during embryonic development, even as it continues to undergo dramatic morphological changes and cellular differentiation. Fast and high resolution three-dimensional (3D) imaging is needed to document the intrinsic